Budding Transition for Bilayer Fluid Vesicles with Area-Difference Elasticity

U. Seifert, L. Miao, H.-G. Döbereiner, and M. Wortis

Department of Physics, Simon Fraser University,
Burnaby, BC, Canada, V5A 1S6

Abstract. We consider a curvature model for bilayer vesicles with an area-difference elasticity or non-local bending-energy term. Such a model interpolates between the bilayer-couple and spontaneous-curvature models. We report preliminary results for the budding transition. The shape transformation between the dumbbell and the pear phases can be continuous or discontinuous depending on the ratio of the non-local to the local bending rigidities.

1. The model

Vesicles exhibit an amazing variety of different shapes. Transformations between these shapes can be induced by changing external parameters such as temperature or osmotic conditions. Our understanding of these phenomena is largely based on the analysis of simple curvature models [1]. In these models the vesicle is described as a two-dimensional surface whose shape is determined by minimizing an appropriate curvature energy under constraints on the enclosed volume V and the total area $A \equiv 4\pi R^2$, where R defines a length scale. Two such models have been studied so far in some detail: (i) In the bilayer-couple or area-difference (ΔA-) model [2,3], the curvature energy is given by

$$G = (\kappa/2) \oint dA(C_1 + C_2)^2, \tag{1}$$

where C_1 and C_2 are the two principal curvatures and κ is the local bending rigidity. In addition, the shape is subject to a constraint on the area difference $\Delta A \approx D \oint dA(C_1 + C_2)$ between the inner and outer monolayers, which have a separation D. (ii) In the spontaneous-curvature (SC-) model [4], the latter constraint is dropped but in the curvature energy (1) $(C_1 + C_2)$ is replaced by $(C_1+C_2-C_0)$, where C_0 is a spontaneous curvature. The two models are related by a Legendre transformation and have, therefore, the same stationary shapes but rather different phase diagrams, which have recently been investigated systematically [5,6]. At present, experiments [7-9] favour the bilayer-couple approach; but, there are still discrepancies between experiment and theory, which are critically reviewed in Refs. 8-10.

Both models can be considered as special cases of a more general curvature model which reads,

$$F = (\kappa/2) \oint dA(C_1 + C_2 - C_0)^2 + (\kappa'\pi/2AD^2)(\Delta A - \Delta A_0)^2. \tag{2}$$

Springer Proceedings in Physics, Vol. 66 The Structure and Conformation of Amphiphilic Membranes
Editors: R. Lipowsky · D. Richter · K. Kremer

The second term formally attributes an elastic energy to deviations of the area difference ΔA from an unstretched equilibrium value ΔA_0. This term has been derived long ago from the bending of two unconnected monolayers, which leads to this "non-local bending resistence" [11], compare also Refs. 12 and 13. Using elastic models for the two monolayers, these derivations show that the non-local bending rigidity κ' has the same order of magnitude as κ. Therefore, (2) might be considered more realistic than the ΔA- or SC-models, which are recovered for $\kappa' = \infty$ or $\kappa' = 0$, respectively. Minimization of (2) for fixed A and V leads, again, to the same stationary shapes as the two original models. Indeed, there is a simple mapping between the ΔA-model and the model (2), which is most conveniently expressed in dimensionless variables, $m \equiv \Delta A/(2RD), m_0 \equiv \Delta A_0/(2RD), c_0 \equiv C_0 R$, and the dimensionless ratio of the two bending rigidities $\alpha \equiv \kappa'/\kappa$: Every stationary shape in the ΔA-model with reduced area difference m and energy $G(m)$ is also a stationary shape in model (2) for

$$m_0 = m + (G'/\kappa - 2c_0)/\alpha, \tag{3}$$

where $G' \equiv \partial G/\partial m$ denotes the derivative of the curvature energy (1) in the ΔA-model along the branch of stationary shapes at fixed A and V. This condition follows from the variation of (2) with respect to ΔA. Thus, the knowledge of the energy G as a function of m in the ΔA-model allows, in principle, a derivation of the phase diagram for (2), which depends on the four variables, α, c_0, m_0, and the reduced volume $v \equiv V/(4\pi R^3/3)$.

2. The budding transition

In this contribution, we report preliminary results [14] for the part of the phase diagram of model (2) where budding occurs. This shape transformation involves up/down symmetric prolate shapes or "dumbbells", up/down asymmetric "pears" and fully vesiculated shapes with necks of microscopic diameter. Experimentally, the symmetry-breaking transition has been reported both as a continuous transition [7] and as a discontinuous transition from prolates to vesiculated shapes without pear-shaped intermediates [9]. In addition, even if the symmetry breaking is continuous and leads to stable pears, there is some evidence for a discontinuous shrinkage of the neck and irreversibility (hysteresis) in the final vesiculation process [8,9].

For the model (2), the relevant part of the three-dimensional phase diagram for a typical (fixed) reduced volume ($v = 0.8$) is shown in Fig. 1. This phase diagram is obtained by using the mapping (3) and the energy $G(m)$ of the dumbbells and pears, as displayed in Fig. 4 of Ref. 6 (with $m = 4\pi\Delta a$). For $\alpha = \infty$, which corresponds to the ΔA-model, the transition or bifurcation between the dumbbells and the pears is continuous at $m_0 = m_C$, independent of c_0. With decreasing α, this transition remains continuous and is given by $m_0 = m_C + (G'_C/\kappa - 2c_0)/\alpha$, where the subscript C refers to the bifurcation point in the ΔA-model. The local topology of the bifurcation is preserved as long as the mapping (3) is monotonic. On further decreasing α, it becomes

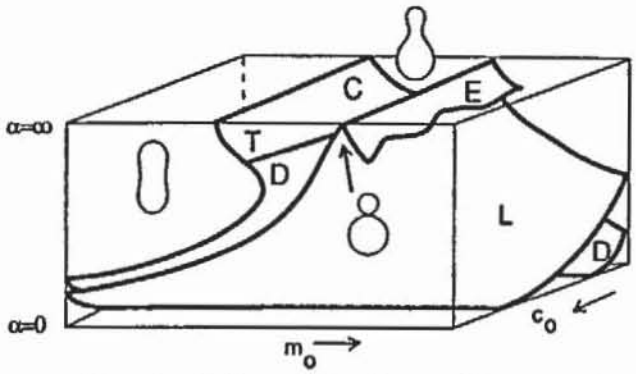

Fig. 1: Schematic phase diagram for model (2) at fixed reduced volume $v = 0.8$. The sheets C and D denote continuous and discontinuous transitions between the dumbbells and the pears. These sheets are separated by the tricritical line T. The sheet L marks the continuous transition to the vesiculated shape consisting of two spheres. For large $\alpha < \infty$ these shapes have a finite region of existence bounded by the sheet E, which denotes the transition to a sphere-plus-ellipse shape.

non-monotonic (first at the bifurcation point) if $\alpha < \alpha_T \equiv -G''_C/\kappa$, where $G''_C < 0$ denotes the second derivative of the energy G along the pear-shaped branch at the bifurcation point. This leads to a wing [6] in the $F(m_0)$-curve and, thus, to a discontinuous transition between the dumbbells and the pears for $\alpha < \alpha_T$. Therefore, $\alpha = \alpha_T (\simeq 2.5$ for $v = 0.8)$ corresponds to a tricritical line independent of c_0 (which becomes a tricritical surface $\alpha_T(v)$ in the full four-dimensional phase diagram). The smaller α the more pronounced becomes the first-order transition. At $\alpha = 0$, one recovers the discontinous transition of the SC-model independent of m_0.

Consider now the transition from the pear to the limiting (L), fully vesiculated shape, which consists of two spheres sitting on top of each other connected by a narrow neck. In the ΔA-model the pears approach this limit continuously as m_0 is increased. Due to its geometrical constraints, such a shape requires a particular $m_0 = m_L$ in the ΔA-model. For $m_0 > m_L$, the fully vesiculated shapes consist of an ellipse and a sphere connected by an infinitesimal neck. For $\alpha < \infty$ the limit shape with the two spheres exists over a finite range of m_0-values, the width of which scales like $\sim 1/\alpha$ (compare Fig. 1). However, with decreasing α additional first-order transitions to vesiculated shapes with more necks or consisting of more complicated segments (such as a dumbbell on top of a sphere) become relevant.

In conclusion, the order of the budding transition and the sequence of vesiculated shapes depends crucially on the ratio of the two bending rigidities. In order to correlate the theoretical results with the various experimental findings beyond mere fitting, an independent measurement of the non-local bending rigidity is required.

Acknowledgments. We thank E. Evans, W. Helfrich, R. Lipowsky and E. Sackmann for informative discussions. This work was funded by the National Science and Engineering Research Council of Canada.

References

[1] For a general review and a comprehensive list of references, see R. Lipowsky, *Nature* **349**, 475, 1991.
[2] E. Evans, *Biophys. J.* **30**, 265, 1980.
[3] S. Svetina, B. Zeks, *Biomed. Biochim. Acta* **42**, 86, 1983.
[4] W. Helfrich, *Z. Naturforsch.* **28c**, 693, 1973.
[5] L. Miao, B. Fourcade, M. Rao, M. Wortis, and R.K.P. Zia, *Phys. Rev. A* **43**, 6843, 1991.
[6] U. Seifert, K. Berndl, and R. Lipowsky, *Phys. Rev. A* **44**, 1182, 1991.
[7] K. Berndl, J. Käs, R. Lipowsky, E. Sackmann, and U. Seifert, *Europhys. Lett.* **13**, 659, 1990.
[8] H.G. Döbereiner, W. Rawicz, M. Wortis, and E. Evans, preprint.
[9] J. Käs and E. Sackmann, *Biophys. J.*, to be published.
[10] M. Wortis, U. Seifert, K. Berndl, B. Fourcade, L. Miao, M. Rao, and R.K.P. Zia, in *Proceedings of the workshop on "Dynamical phenomena at interfaces, surfaces and bilayers"*, edited by D. Beysens, N. Boccara and G. Forgacs.
[11] E. Evans, *Biophys. J.* **14**, 923, 1974.
[12] W. Helfrich, *Z. Naturforsch.* **29c**, 510, 1974.
[13] S. Svetina, M. Brumen, and B. Zeks, *stud. biophysica* **110**, 177, 1985.
[14] H.G. Döbereiner, L. Miao, U. Seifert, and M. Wortis, to be published.